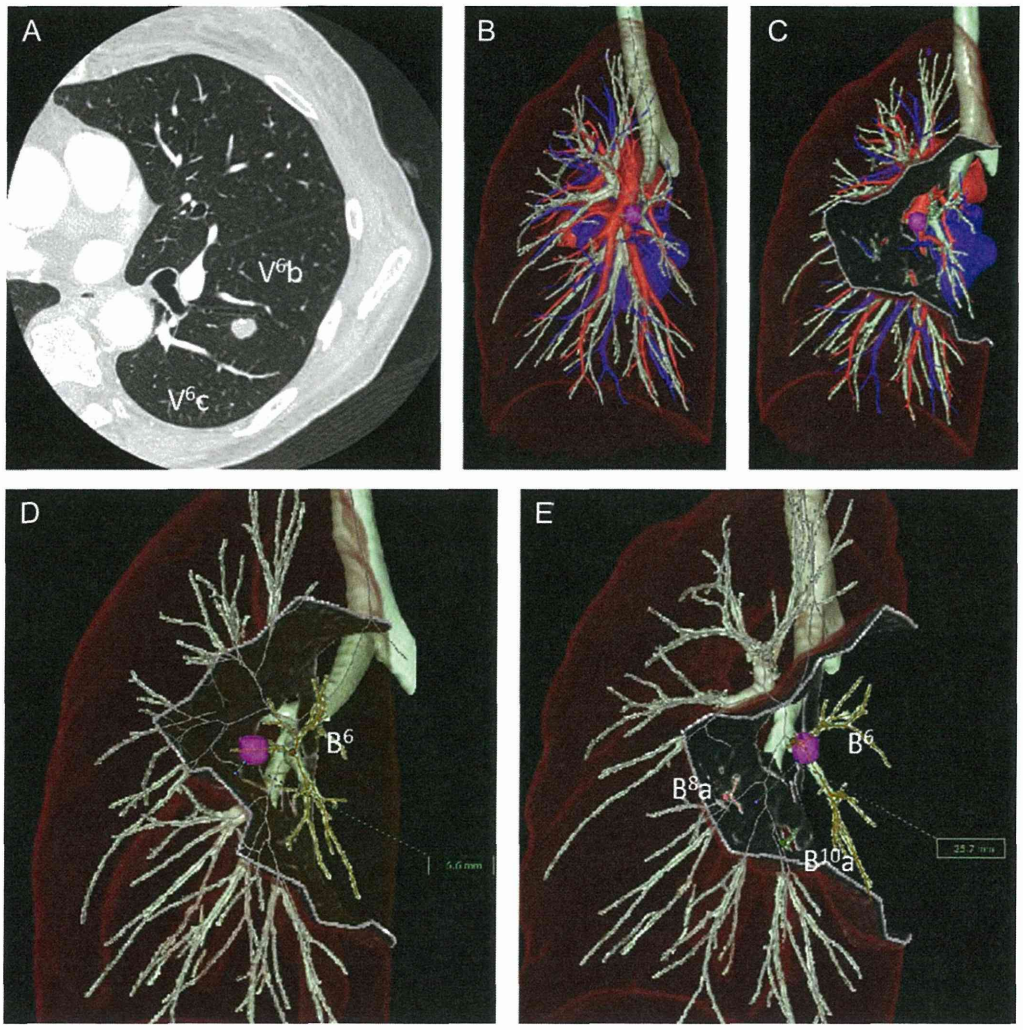

Figure 2: Case 1 (**A** and **B**). According to the virtual S6 segmentectomy, the surgical margin would be estimated to be only 6.6 mm (**D**). While in the virtual segmentectomy of left S6 + S8a + S10a, the appropriate surgical margin was 25.7 mm (**C** and **E**). V^6: superior lower vein, B^6: superior lower bronchus, B^{10}: posterior basal bronchus.

inter-segmental plane. After the segmental bronchi were isolated and dissected using staples or 2-0 silk sutures. Electrocauterization was used to divide the inter-segmental plane along the inflation–deflation line from the peripheral site to the hilum. At the central portion around the hilum, the inter-segmental plane was approached along the inter-segmental vein. We also guided the visualization of 3D CT imaging, including the segmental surface based on virtual segmentectomy simulation to obtain accurate surgical margins. Staplers were only used to divide the inter-segmental plane when the lung was emphysematous, to minimize air leakage. The dissected raw parenchymal surface was sealed with a commercially available fibrin sealant and a bioabsorbable polyglycolic acid felt.

CLINICAL EXPERIENCE

When first using this surgical simulation and navigation system for segmentectomy, we attempted this novel technique on 3 cases of pulmonary metastases and 1 of multiple lung cancer (Table 1). Here, we describe 2 representative cases.

Case 1 was a 69-year old woman with a small solitary pulmonary nodule. Her previous history was mesopharyngeal carcinoma treated with surgical resection followed by chemoradiotherapy 1 year previously. Chest CT scanning revealed a suspicious metastatic pulmonary tumour located in the superior segment of the left lower lobe (S6) (Fig. 2A). This tumour was very close to pulmonary veins V^6b and V^6c, which are supposed to be inter-segmental pulmonary veins between S6 and the basal segment of the left lower lobe (Fig. 2A). If only the superior segmentectomy of the left lower lobe was performed in this case, this surgical margin was estimated at 6.6 mm, which is <2.0 cm or the maximum tumour size based on the result of the virtual segmentectomy of the superior segment of the left lower lobe (Fig. 2D). Therefore, we performed the extended superior segmentectomy of the left lower lobe according to the preoperative simulation of the virtual segmentectomy of left S6 + S8a + S10a, obtaining an appropriate surgical margin (25.7 mm), >2.0 cm or the maximum diameter of this tumour (8.8 mm) (Fig. 2E) [6].

Case 2 was a 43-year old man with a 21.2-mm solitary pulmonary nodule in the left S9 + 10 basal segment of the left lower lobe. He had undergone thyroidectomy and thymectomy for thyroid carcinoma and thymic carcinoma 3 and 2 years previously, respectively. This tumour was located on the exact line between S9 and S10 according to the 3D imaging reconstruction

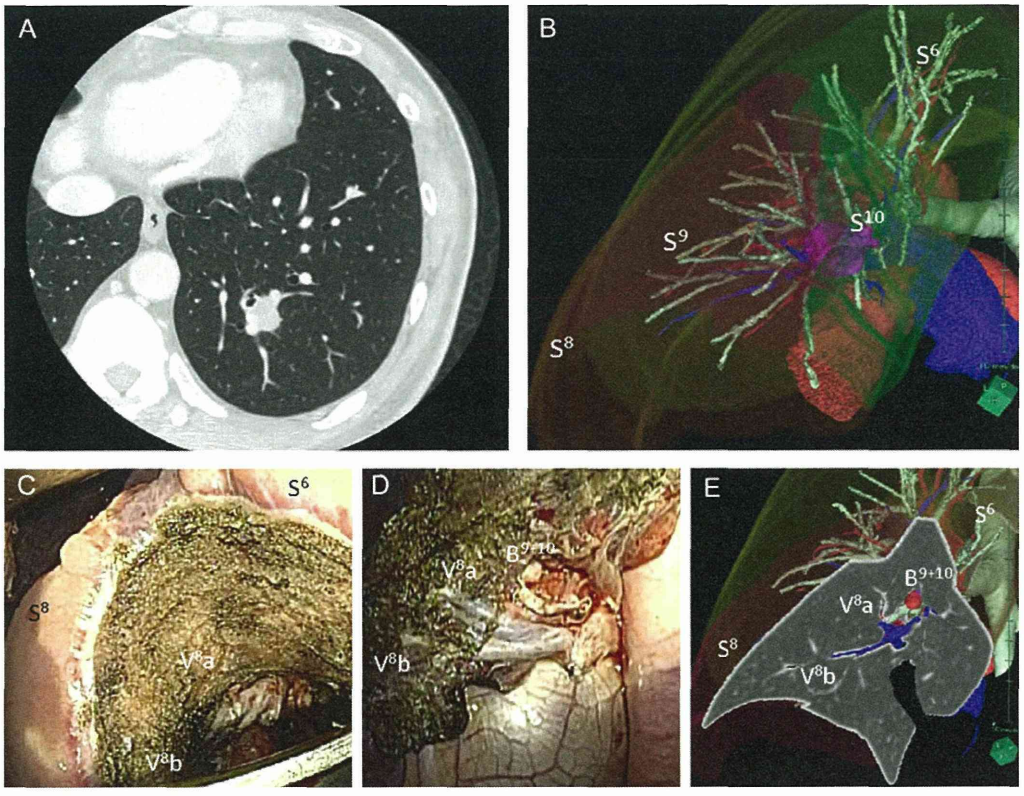

Figure 3: Case 2 (**A** and **B**). Left S9 + S10 segmentectomy under visual guidance of the appropriate virtual segmentectomy (**C–E**). S^{6}: superior, lower lobe, S^{8}: anteromedial basal segment, S^{9}: lateral basal segment, S^{10}: posterior basal segment, V^{8}: anterior basal pulmonary vein, B^{9+10}: lateral and posterior basal bronchi.

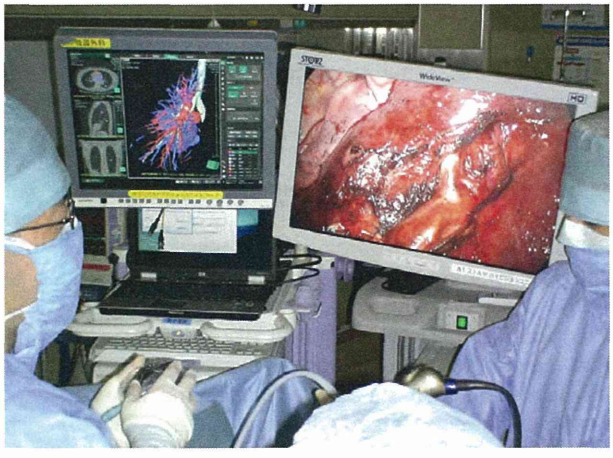

Figure 4: Thoracoscopic surgery using the double monitor guidance system. The thoracoscopy television monitor (right) and the 3D imaging system (left).

of each segmental area of the left lower lobe (Fig. 3B). Therefore, we performed a left S9 + S10 segmentectomy under visual guidance of the appropriate virtual segmentectomy. We used an electrocautery Bovie to dissect the lung parenchyma along the line between inflated and deflated lung, visually guided by the visualization of 3D CT imaging, based on virtual segmentectomy simulation to obtain accurate surgical margins (Fig. 3C–E).

Table 1 shows the preliminary results of surgical outcomes in our 4 consecutive cases. We performed three complex segmentectomies: an extended left S6 segmentectomy, a left S9 + S10 segmentectomy and a right S7 + S8 segmentectomy. We also performed one moderate segmentectomy: a basal segmentectomy of the right lower lobe. After the lung parenchyma was dissected, we sealed it with a commercially available fibrin sealant and a bioabsorbable polyglycolic acid felt in 3 of 4 cases. Operation times were all within 4 h, blood loss volumes ranged from 24 to 120 ml, and chest tubes could be removed on POD 3 in all patients. The durations of hospitalization were from POD 5 to POD 9 without moderate or severe postoperative complications. According to comparisons between 3D CT imaging and pathological findings (Table 2), the extents of preoperative predicted surgical margins by Synapse Vincent tended to be shorter than those of pathological surgical margins, because of deflated resected lung lobes. However, there were no residual tumour cells at the surgical resection margins (confirmed pathologically) and no local recurrence could be detected in any of the 4 cases during the short follow-up period (15–17 months).

COMMENT

The efficacy of 3D CT angiography using MDCT for preoperative assessment for thoracic surgery has been described. Accuracy in depicting individual anatomies of pulmonary vessels and bronchi and preoperative simulation using 3D CT could play an important role in facilitating a safe and complete VATS lobectomy procedure, as has been suggested in some previous reports. Fukuhara *et al.* reviewed 49 consecutive patients with clinical stage I lung cancer and compared intraoperative findings of the pulmonary artery branching pattern with 3D CT angiography images preoperatively obtained using MDCT. According to the results, 95.2% of the pulmonary artery branches were precisely

Table 1: Patient characteristics and surgical outcomes

Case	Age (years)	Sex	Diagnosis	Location	Tumour size (mm)	Operation procedure	Inter-segment	Operation time	Blood loss (ml)	Duration of chest tube placement (POD)	Duration of hospitalization	Morbidity
1	69	F	PM from mesopharyngeal carcinoma	Rt S6	8.8	Lt S6 segmentectomy	Electrocautery	3 h 39 m	120	3	7	None
2	43	M	PM from thymic carcinoma	Lt S9	21.2	Lt S9 + S10 segmentectomy	Electrocautery	3 h 09 m	24	3	9	None
3	77	F	Multiple lung cancer	Rt S8	13.0	Rt S7 + S8 segmentectomy	Electrocautery	3 h 42 m	68	3	5	None
4	59	M	PM from rectal cancer	Rt S9	19.8	Rt basal segmentectomy	Stapler	3 h 52 m	70	3	5	None

Lt: left; PM: pulmonary metastasis; POD: postoperative days; Rt: right.

identified on preoperative 3D CT angiography and conversion to open thoracotomy was not needed. Watanabe *et al.* also reviewed 14 lung cancer cases and stated that 3D CT pulmonary artery navigation may have the potential to increase the safety of surgical procedures [7, 8]. Recently, preoperative identification of the inter-segmental pulmonary vessels and bronchi involved with the resected segment using 3D CT angiography and establishment of a virtual bronchial tree (virtual bronchography) have been demonstrated to be useful tools, enabling the surgeon to perform an accurate anatomical segmentectomy [9, 10]. However, to the best of our knowledge, identifying the inter-segmental surface and calculating appropriate surgical margins by this method have never been established for preoperative procedures for segmentectomy. This article is apparently the first report demonstrating the efficacy of virtual segmentectomy.

It is critical to identify the inter-segmental veins as the boundary lines of the pulmonary segments to determine the lateral surgical margins and to identify the target segmental bronchi as the vertical surgical margins before segmentectomy. However, given the many anatomical variations of pulmonary veins and bronchi, it is difficult to identify the intra-segmental and inter-segmental veins and target segmental bronchi, even by using 3D CT angiography and virtual bronchography. Moreover, it is technically difficult to perform a typical segmentectomy because of the tumour location (Cases 1 and 2). Recently, we have occasionally encountered cases which required multi-segmentectomy for several tumours. Therefore, we have developed the novel segmentectomy simulation system based on high-quality 3D lung modelling from MDCT imaging using the specially developed Synapse Vincent software in collaboration with Fujifilm Corporation.

This particular system consist of the following three novel functions: (i) calculation of the bronchial ventilation area using the algorithm based on the direction and diameter of the bronchi; (ii) visualization of the segmental surface resulting in determination of resected pulmonary artery, vein, bronchi and inter-segmental veins and (iii) calculation of the length of the surgical margin. Based on the preliminary results of our cases, we believe that it could be useful for appropriate anatomical segmentectomy with curative resection. It would enable one to obtain accurate preoperative information regarding not only the relationships among the tumour, the intra-segmental and inter-segmental veins, the target segmental bronchi and pulmonary arteries, but also to visualize the inter-segmental plane surface and secure surgical margins. Moreover, intraoperative visualization guidance of the inter-segmental surface, including intra-segmental and inter-segmental veins, target pulmonary arteries, and bronchi could help thoracic surgeons perform accurate anatomical segmentectomy and curative resection. Additional applications of this novel system include preoperative simulation of multi-segmentectomy for synchronous or metachronous multiple pulmonary tumours and visual guidance for robotic surgeries.

In this preliminary study, we first attempted to demonstrate the usefulness of virtual segmentectomy based on high-quality 3D lung modelling from conventional multidetector CT images to compare intraoperative findings of the pulmonary artery, pulmonary vein and bronchial branching patterns and visualization of the segmental surface. Therefore, we basically performed hybrid VATS to make an accurate assessment not only on a television monitor that provides a 2D view, but also for direct observation using mini-thoracotomy with a real 3D view. In our next study, we will perform complete VATS segmentectomy using this novel technology.

Table 2: Comparisons between 3D CT imaging and pathological findings

Case	Vincent tumour size (CT) (mm)	Pathological tumour size (mm)	Vincent surgical margin length (mm)	Pathological surgical margin length (mm)	Pathological surgical margin	Follow-up (months)	Local recurrence
1	8.8	11.0	12.4	9.8	Negative	14	None
2	21.2	20.0	15.0	10.0	Negative	14	None
3	13.0	13.0	20.6	12.0	Negative	13	None
4	19.8	18.0	30.0	25.0	Negative	12	None

It is critical to obtain an adequate surgical margin for pulmonary malignant tumours, particularly for primary lung cancer. The Vincent surgical margins are overestimated, as evidenced by the pathological margins (Table 2). As this is a preliminary study with a small number of sample cases, we are currently evaluating more cases and assessing detailed information. Because we are more familiar with using this novel technology and performing segmentectomy in many cases with much more inflated target segments, the discrepancies between the Vincent surgical margin and the pathological surgical margin is decreasing.

We understand that a major limitation remains in this system. Virtual visualization of the segmentectomy resection line consisted of the border of the inflated lung, whereas the lung was, in reality, deflated during actual surgical procedures. Further technical development is needed to improve this limitation.

We describe the benefit of virtual segmentectomy, a novel surgical simulation system based on high-quality 3D lung modelling, including vascular and bronchial structures. Preoperative determination of the branches of the pulmonary vessels and segmental bronchi branches and the anatomical inter-segmental surface estimated by the inflated area of segmental bronchi is possible by visualization. Moreover, a sufficient surgical margin from the tumour can be estimated. This new technology appears useful for thoracic surgeons to perform appropriate anatomical segmentectomy and curative resection. Furthermore, we are currently performing a prospective clinical study to demonstrate the efficacy of this novel system for small peripheral primary lung cancer lesions.

ACKNOWLEDGEMENTS

We are indebted to Clifford A. Kolba, Edward F. Barroga and J. Patrick Barron, Department of International Medical Communications of Tokyo Medical University, for their editorial review of the English manuscript.

FUNDING

This study was supported by a Grant-in-Aid for Scientific Research, Japan Society for the Promotion of Science (24592104), and Ministry of Education, Culture, Sports, Science and Technology, Japan.

Conflict of interest: Hisashi Saji and Norihiko Ikeda have given remunerated lectures for Fujifilm. No author received research funding and all had full control of the study design, methods used, outcome parameters, data analysis and production of the written report.

REFERENCES

[1] Sakata R, Fujii Y, Kuwano H. Thoracic and cardiovascular surgery in Japan during 2009: annual report by the Japanese Association for Thoracic Surgery. Gen Thorac Cardiovasc Surg 2011;59:636–67.
[2] Yamanaka J, Saito S, Fujimoto J. Impact of preoperative planning using virtual segmental volumetry on liver resection for hepatocellular carcinoma. World J Surg 2007;31:1249–55.
[3] Saito S, Yamanaka J, Miura K, Nakao N, Nagao T, Sugimoto T *et al.* A novel 3D hepatectomy simulation based on liver circulation: application to liver resection and transplantation. Hepatology 2005;41:1297–304.
[4] Lang H, Radtke A, Hindennach M, Schroeder T, Fruhauf NR, Malago M *et al.* Impact of virtual tumor resection and computer-assisted risk analysis on operation planning and intraoperative strategy in major hepatic resection. Arch Surg 2005;140:629–38; discussion 638.
[5] Yamanaka J, Saito S, Iimuro Y, Hirano T, Okada T, Kuroda N *et al.* The impact of 3-D virtual hepatectomy simulation in living-donor liver transplantation. J Hepatobiliary Pancreat Surg 2006;13:363–9.
[6] Sawabata N, Ohta M, Matsumura A, Nakagawa K, Hirano H, Maeda H *et al.* Optimal distance of malignant negative margin in excision of non-small cell lung cancer: a multicenter prospective study. Ann Thorac Surg 2004;77:415–20.
[7] Watanabe S, Arai K, Watanabe T, Koda W, Urayama H. Use of three-dimensional computed tomographic angiography of pulmonary vessels for lung resections. Ann Thorac Surg 2003;75:388–92; discussion 392.
[8] Fukuhara K, Akashi A, Nakane S, Tomita E. Preoperative assessment of the pulmonary artery by three-dimensional computed tomography before video-assisted thoracic surgery lobectomy. Eur J Cardiothorac Surg 2008;34:875–7.
[9] Oizumi H, Endoh M, Takeda S, Suzuki J, Fukaya K, Sadahiro M. Anatomical lung segmentectomy simulated by computed tomographic angiography. Ann Thorac Surg 2010;90:1382–3.
[10] Shimizu K, Nakano T, Kamiyoshihara M, Takeyoshi I. Segmentectomy guided by three-dimensional computed tomography angiography and bronchography. Interact CardioVasc Thorac Surg 2012;15:194–6.

OncoTargets and Therapy

Dovepress

open access to scientific and medical research

Open Access Full Text Article

ORIGINAL RESEARCH

Cancer stem cell-related marker expression in lung adenocarcinoma and relevance of histologic subtypes based on IASLC/ATS/ERS classification

Yoshihisa Shimada[1]
Hisashi Saji[3]
Masaharu Nomura[1,2]
Jun Matsubayashi[2]
Koichi Yoshida[1]
Masatoshi Kakihana[1]
Naohiro Kajiwara[1]
Tatsuo Ohira[1]
Norihiko Ikeda[1]

[1]Department of Surgery I, [2]Department of Anatomic Pathology, Tokyo Medical University Hospital, Tokyo, Japan; [3]Department of Chest Surgery, St Marianna University School of Medicine, Kawasaki, Japan

Background: The cancer stem cell (CSC) theory has been proposed to explain tumor heterogeneity and the carcinogenesis of solid tumors. The aim of this study was to clarify the clinical role of CSC-related markers in patients with lung adenocarcinoma and to determine whether each CSC-related marker expression correlates with the histologic subtyping proposed by the International Association for the Study of Lung Cancer (IASLC), the American Thoracic Society (ATS), and the European Respiratory Society (ERS) classifications.

Methods: We reviewed data for all 103 patients in whom complete resection of adenocarcinoma had been performed. Expression of CSC-related markers, ie, aldehyde dehydrogenase 1A1 (ALDH1A1), aldo-keto reductase 1C family member 1 (AK1C1), and 1C family member 3 (AK1C3), was examined using immunostaining on whole-mount tissue slides, and the tumors were reclassified according to the IASLC/ATS/ERS classification.

Results: ALDH1A1 expression was observed in 66.0% of tumors, AK1C1 in 62.7%, and AK1C3 in 86.1%. Immunoreactivities with the frequency of mean expression of ALDH1A1 in papillary predominant adenocarcinoma were significantly higher than those of solid predominant adenocarcinoma ($P<0.05$). Papillary predominant adenocarcinoma had significantly lower expression of AK1C1 when compared with noninvasive or solid predominant adenocarcinomas ($P<0.05$). On multivariate analysis, larger tumor size (hazards ratio 1.899, $P=0.044$), lymph node metastasis (hazards ratio 2.702, $P=0.005$), and low expression of ALDH1A1 (hazards ratio 3.218, $P<0.001$) were shown to be independently associated with an unfavorable prognosis.

Conclusion: Immunohistochemistry of ALDH1A1 expression is strongly associated with prognosis. Expression of each CSC-related marker varies according to subtype, suggesting that a comprehensive histologic subtyping approach in the IASLC/ATS/ERS classification provides new molecular biology insights into the genesis of lung adenocarcinoma according to CSC theory.

Keywords: cancer stem cell marker, adenocarcinoma, ALDH1A1, AK1C1, AK1C3, prognosis

Introduction

Lung cancer is the most lethal of all cancers, and adenocarcinoma (ADC) is the most common histopathologic type of lung cancer worldwide.[1] Major advances in ADC management have resulted from the understanding of molecular biology, development of molecular targeting agents, and identification of biomarkers for targeted treatment. However, there exists a widely divergent clinical, radiologic, molecular and pathologic spectrum in lung ADC. In this context, the International Association for the Study of Lung Cancer (IASLC), the American Thoracic Society (ATS), and the European Respiratory Society (ERS) have proposed a new subclassification of lung ADCs that relies on the predominant structural morphology.[2] Histologic subtyping according to

Correspondence: Yoshihisa Shimada
Department of Surgery I, Tokyo Medical University, 6-7-1 Nishishinjuku, Shinjuku-ku, Tokyo, 160-0023, Japan
Tel +81 03 3342 6111
Fax +81 03 3342 6203
Email zenkyu@za3.so-net.ne.jp

submit your manuscript | www.dovepress.com
Dovepress
http://dx.doi.org/10.2147/OTT.S52353

© 2013 Shimada et al. This work is published by Dove Medical Press Limited, and licensed under Creative Commons Attribution – Non Commercial (unported, v3.0) License. The full terms of the License are available at http://creativecommons.org/licenses/by-nc/3.0/. Non-commercial uses of the work are permitted without any further permission from Dove Medical Press Limited, provided the work is properly attributed. Permissions beyond the scope of the License are administered by Dove Medical Press Limited. Information on how to request permission may be found at: http://www.dovepress.com/permissions.php

the IASLC/ATS/ERS classification has been reported to have a strong relationship with prognosis in several studies.[3–7]

Cancer stem cell (CSC) theory has been proposed to explain tumor heterogeneity and the carcinogenesis of solid tumors, including lung cancer.[8] CSCs, a very small population of specialized cells, have potential for self-renewal and extensively proliferative characteristics that sustain tumor formation.[8,9] Various molecules are being investigated as putative markers of CSCs. In this study, we focused on aldehyde dehydrogenase 1A1 (ALDH1A1), aldo-keto reductase 1C family member 1 (AK1C1), and 1C family member 3 (AK1C3), which have been previously identified as labeling CSCs in breast, colon, prostate, and lung cancer.[10–15] In particular, ALDH1 has already been evaluated as an effective prognostic marker in lung cancer.[12,15,16]

In the current study, we attempted to determine whether expression of each CSC-related marker is correlated with the IASLC/ATS/ERS classification, and whether expression of CSC-related markers has any bearing on overall survival.

Materials and methods

Patients

The subjects recruited for this study consisted of 103 patients with lung ADC who underwent complete surgical resection at Tokyo Medical University Hospital between December 1999 and January 2002. All of these patients underwent complete lobar resection and systematic mediastinal lymph node dissection. We excluded patients who had undergone preoperative chemotherapy or radiotherapy. Diagnoses were made according to the criteria of the current World Health Organization classification for lung cancer and the IASLC/ATS/ERS international multidisciplinary classification of lung ADC.[2] The 7th edition International Union Against Cancer/American Joint Committee on Cancer TNM classification was applied to all ADCs.[17] Data collection and analyses were approved, and the need to obtain written informed consent from each patient was waived by the Tokyo Medical University institutional review board.

Clinical characteristics were retrieved from the clinical records available. The following clinicopathologic factors were assessed retrospectively in relation to immunohistochemical analysis: age, gender, smoking history, pathologic staging, tumor size, pathologic nodal involvement, grade of differentiation, vascular invasion, and pleural invasion.

Histopathology

After the specimens were fixed with formalin and embedded in paraffin, serial 4 μm sections were stained with hematoxylin and eosin and by the Alcian Blue-periodic acid-Schiff method to visualize cytoplasmic mucin and by the Elastica van Gieson method to visualize elastic fibers. All slides were evaluated by three of the authors (YS, MN, JM) together using a multiheaded microscope and discussed until consensus was achieved.

All tumor areas were evaluated on the slides. If several tumor foci were present, all foci were included in the analysis. Evaluation was done according to the criteria of the IASLC/ATS/ERS classification, recording the percentage of each histologic component in 5% increments: adenocarcinoma in situ (Figure 1A), minimally invasive adenocarcinoma (Figure 1B), lepidic and acinar (Figure 1C), solid (Figure 1D), papillary, micropapillary (Figure 1E), and mucinous predominant (Figure 1F). The predominant pattern was defined as the pattern with the largest area percentage.

Immunohistochemistry

Expression of three CSC-related proteins was tested with the following commercially available antibodies according to the respective manufacturer's protocols: monoclonal rabbit anti-ALDH1A1 antibody (Abcom Japan, Tokyo, Japan), polyclonal anti-AK1C1 antibody (GeneTex, Irvine, CA, USA), and monoclonal anti AK1C3 antibody (Sigma Japan, Tokyo, Japan). Sections were briefly incubated with xylene, rehydrated with graded ethanol solutions, and incubated with methyl alcohol containing 3% hydrogen peroxide to remove endogenous peroxidase activity. After washing thoroughly with phosphate-buffered saline, sections were incubated with adequately diluted primary antibodies and then with Histofine® simple stain (Nichirei Bioscience, Tokyo, Japan), and finally visualized with products of the peroxidase and diaminobenzidine reaction.

Antibody binding was microscopically recognizable as brown cytoplasmic staining. We categorized immunoreactivity by the percentage of the immunopositive area. In tumor cells of interest, when more than 5% of the staining extensiveness showed an unequivocally strong reaction with an antibody, the tumor was classified as positive.

Statistical analysis

Overall survival was measured from the date of surgery to the date of death from any cause or the date on which the patient was last known to be alive. Survival curves were plotted according to the Kaplan–Meier method and compared using the log-rank test. Categoric comparisons were performed using the Pearson chi-squared test. Multivariate analysis was performed using the Cox proportional hazards model. A

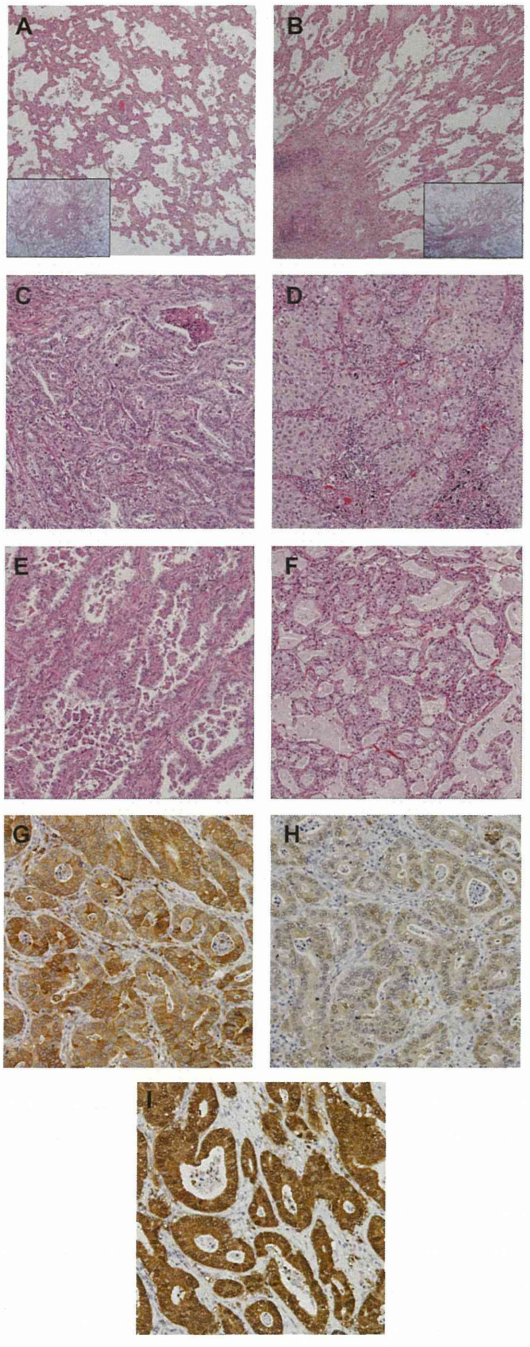

Figure 1 Images of predominant growth patterns and immunohistochemical staining of ALDH1, AK1C1, and AK1C3. (**A**) Adenocarcinoma in situ, (**B**) minimally invasive adenocarcinoma, (**C**) acinar, (**D**) solid, (**E**) micropapillary, and (**F**) mucinous predominant adenocarcinoma. Also shown are immunohistochemical staining images for (**G**) ALDH1A1, (**H**) AK1C1, and (**I**) AK1C3. These slides correspond to the acinar predominant adenocarcinoma shown in Figure 1C.
Abbreviations: ALDH1A1, aldehyde dehydrogenase 1A1; AK1C1, aldo-keto reductase 1C family member 1; AK1C3, aldo-keto reductase 1C family member 3.

one-way analysis of variance, with the Tukey-Kramer multiple comparison post hoc test, was used to allow for unequal sample sizes and determine whether there was a significant difference between the mean immunohistochemical extensiveness according to the predominant histologic pattern of ADC. A P-value of less than 0.05 was considered to indicate a statistically significant difference. The Stat-view 5.0 software package was used to perform the statistical analysis (SAS Institute Inc., Cary, NC, USA).

Results

Predominant growth pattern and ALDH1A1, AK1C1, and AK1C3 expression

All resected specimens were reclassified according to the IASLC/ATS/ERS classification. Representative results are shown in Figure 1. Reclassification of the 103 specimens resulted in three adenocarcinoma in situ (2.9%, Figure 1A), six minimally invasive adenocarcinoma (5.8%, Figure 1B), and 94 invasive ADCs (91.3%). Invasive ADCs were further divided into: lepidic predominant, eight (7.8%); papillary predominant, 39 (37.9%); acinar predominant, ten (9.7%, Figure 1C); solid predominant, 27 (26.2%, Figure 1D); and micropapillary predominant, five (4.9%, Figure 1E). Specific ADC subtypes included four invasive mucinous ADCs (3.9%, Figure 1F) and one enteric ADC (1.0%). Representative examples of immunohistochemical stains for ALDH1A1, AK1C1, and AK1C3 are shown in Figure 1G–I, respectively. This corresponds to the acinar predominant ADC shown in Figure 1C. These CSC-related markers were expressed mainly in the cytoplasm and membrane of the tumor cells. Tumor cells in 68 (66.0%) of the 103 specimens were positive for ALDH1A1, tumor cells in 64 (62.7%) were positive for AK1C1, and tumor cells in 87 (86.1%) were positive for AK1C3.

Correlation between CSC-related marker expression and predominant ADC subtypes

We investigated the correlation between expression of ALDH1A1, AK1C1, and AK1C3 and each predominant subtype. Figure 2 presents the immunohistochemical extensiveness results for adenocarcinoma in situ–minimally invasive ADC (noninvasive ADC), lepidic, acinar, solid, papillary, micropapillary, and mucinous ADC. Immunoreactivities with the percentage of immunopositive areas show that the mean expression of ALDH1A1 in papillary predominant ADCs was significantly higher than that in solid predominant ADCs (Figure 2A, $P<0.05$). On the other hand, Figure 2B shows that papillary predominant ADCs had significantly lower expression of AK1C1 compared with noninvasive or solid predominant ADCs ($P<0.05$). No significant

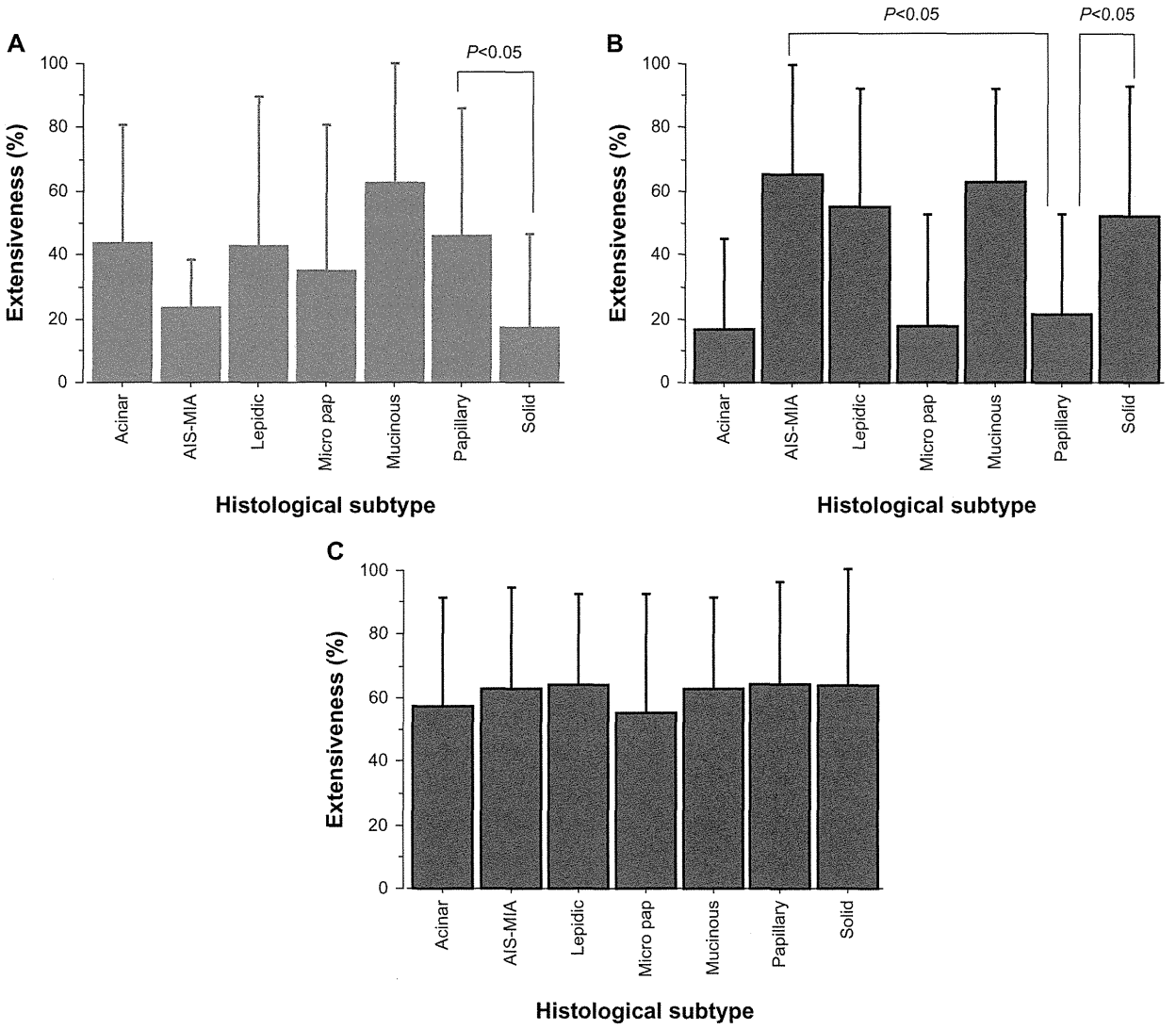

Figure 2 Cancer stem cell-related marker expression in each histologic subtype of lung adenocarcinoma. An overview of the correlation between ALDH1A1, AK1C1, and AK1C3 expression and predominant subtypes is provided. The bars reflect the mean ± standard error of the mean for extensiveness of the immunopositive area for each of the growth patterns. (**A**) Mean expression of ALDH1A1 in papillary predominant adenocarcinomas is significantly higher than that in solid predominant adenocarcinomas ($P<0.05$). (**B**) Papillary predominant adenocarcinomas had significantly lower expression of AK1C1 compared with noninvasive or solid predominant adenocarcinomas ($P<0.05$). (**C**) No significant difference in AK1C3 expression was found for any predominant subtype.

Abbreviations: AIS, adenocarcinoma in situ; MIA, minimally invasive adenocarcinoma; ALDH1A1, aldehyde dehydrogenase 1A1; AK1C1, aldo-keto reductase 1C family member 1; AK1C3, aldo-keto reductase 1C family member 3.

difference in AK1C3 expression was found between any of the predominant subtypes (Figure 2C).

Patient characteristics and survival analyses

The median follow-up for survivors was 8.9 years. Table 1 shows the 5-year overall survival proportions according to clinicopathologic characteristics in 103 patients with lung ADC. On univariate analysis, pathologic stage, tumor size, lymph node involvement, histologic vascular invasion, pleural invasion, and ALDH1A1 immunoreactivity status were found to be significantly associated with survival outcome. The 5-year overall survival proportions of patients with ALDH1A1-positive status and ALDH1A1-negative status were 77.9% and 62.2%, respectively. Patients with an ALDH1A1-positive status had longer overall survival than those with an ALDH1A1-negative status ($P=0.002$, Figure 3), whereas staining with AK1C1 and AK1C3 had no prognostic significance ($P=0.249$ and $P=0.113$, respectively). A multivariate Cox proportional hazards model demonstrated that larger tumor size (hazards ratio 1.899, $P=0.044$), lymph node metastasis (hazards ratio 2.702, $P=0.005$), and low expression of ALDH1A1 immunoreactivity (hazards ratio 3.218, $P<0.001$) were independently associated with unfavorable overall survival (Table 2).

Table 1 Patient characteristics and univariate analysis of overall survival

Variable	Cases, n (%)	5-year OS rate	*P*-value
Overall	103	72.6%	
Age (years, median 65)			
<65	50 (49)	73.6%	
≥65	53 (51)	71.7%	0.416
Gender			
Male	57 (55)	68.0%	
Female	46 (45)	78.3%	0.226
Smoking status			
Smoker	59 (57)	67.8%	
Never smoker	44 (43)	79.2%	0.458
p Stage			
I	78 (76)	83.2%	
II	12 (12)	66.7%	(Stage I
III	11 (11)	27.3%	versus II–IV)
IV	2 (2)	50.0%	<0.001
Tumor size			
≤3.0 cm	61 (59)	80.0%	
>3.0 cm	42 (41)	61.9%	0.006
Lymph node metastasis			
Absent	82 (80)	81.5%	
Present	21 (20)	38.1%	<0.001
Differentiation			
Well or moderate	72 (70)	76.2%	
Poor	31 (30)	61.3%	0.304
IASLC/ATS/ERS classification			
AIS	3 (3)	100%	
MIA	6 (6)	100%	
Lepidic	8 (8)	87.5%	
Papillary	39 (38)	64.1%	
Acinar	10 (10)	100%	
Micropapillary	5 (5)	40.0%	
Solid	27 (26)	66.7%	
Mucinous	4 (4)	100%	
Other (enteric)	1 (1)	100%	
Vascular invasion			
Absent	43 (42)	81.1%	
Present	56 (58)	64.3%	0.001
Pleural invasion			
Absent	82 (80)	79.3%	
Present	21 (20)	45.7%	0.005
Adjuvant chemotherapy			
With	40 (39)	75.0%	
Without	63 (61)	71.1%	0.337
ALDH1A1 expression			
<5% positive cells	35 (34)	62.2%	
≥5% positive cells	68 (66)	77.9%	0.002
AK1C1 expression			
<5% positive cells	38 (37)	71.1%	
≥5% positive cells	64 (63)	74.7%	0.249
AK1C3 expression			
<5% positive cells	14 (14)	61.9%	
≥5% positive cells	87 (86)	74.7%	0.113

Abbreviations: AIS, adenocarcinoma in situ; MIA, minimally invasive adenocarcinoma; OS, overall survival; IASLC, International Association for the Study of Lung Cancer; ATS, American Thoracic Society; ERS, European Respiratory Society; ALDH1A1, aldehyde dehydrogenase 1A1; AK1C1, aldo-keto reductase 1C family member 1; AK1C3, aldo-keto reductase 1C family member 3.

Correlation between clinicopathologic features and ALDH1A1 expression

ALDH1A1 expression status was the most powerful prognostic indicator in this cohort. Therefore, we examined correlations between ALDH1A1-positive cases and clinicopathologic features (Table 3). The ALDH1A1-positive cases were significantly associated with less poorly differentiated ADC (P=0.013). No other clinicopathologic factors were correlated with these cases.

Discussion

We set out to determine whether ALDH1A1 immunoreactivity status was the most powerful independent prognostic factor for overall survival in lung ADC, and expression of each CSC-related marker varied in histologic subtype according to the IASLC/ATS/ERS classification. To the best of our knowledge, the association between CSC-related marker expression and the IASLC/ATS/ERS classification has not been previously investigated in patients for all stages of lung ADC.

The three markers examined in this study have been previously reported as candidate CSC-related markers in different types of tumors. ALDH1 is a detoxifying enzyme responsible for oxidation of intracellular aldehydes. The ALDH isoform, ALDH1A1, has been shown to play a role in drug resistance, and its activity has been used to identify stem-like subsets in human hematopoietic cancers and other solid tumors.[18–25] Previously published studies reported that overexpression of ALDH1A1 correlated with poor prognosis in lung cancer.[12,15] Theoretically, a high proportion of CSCs in the tumor should be associated with an unfavorable prognosis. However, our results show that increased expression of ALDH1A1 correlated with more favorable overall survival, so are very much in conflict with the above mentioned literature. One of the reasons for this discrepancy may lie in the methodologic differences or different cutoff values used for distinguishing between positive and negative CSC-related marker expression. Our method was based on evaluating whole-mount tissue slides and 66% of tumor specimens were ALDH1A1-positive, whereas the results of the previous studies based on tissue microarrays showed only 29%–45% of tumor samples to be positive with a mixture of ADCs and other histology.[12,15] Although the current study population was too small to draw any statistically definite conclusions, the methodology of using tissue microarray may prevent detailed observation and increase the rate of false-negative results. Kahlert et al reported that low immunohistochemical expression of ALDH1 in pancreatic cancer was associated with

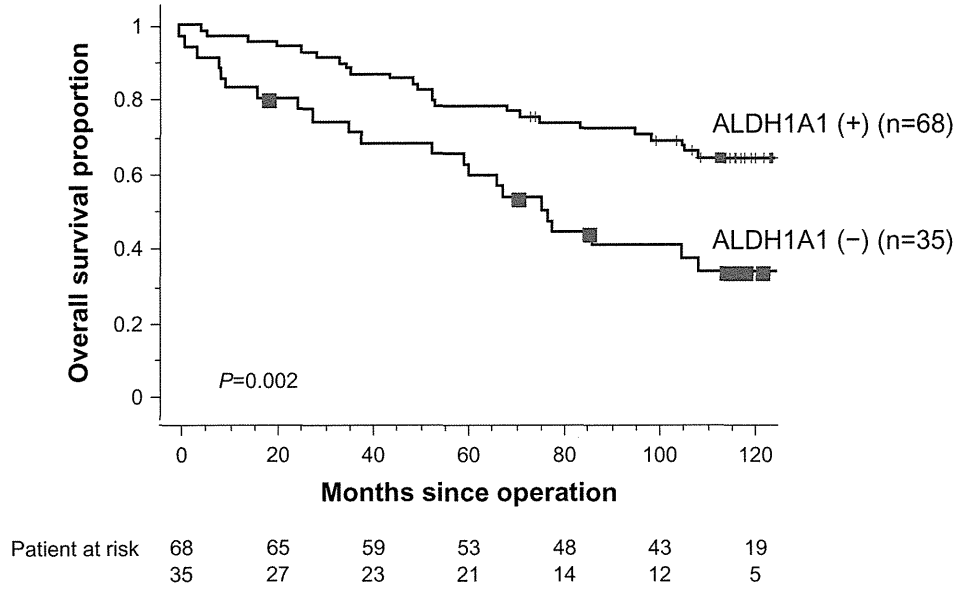

Figure 3 Kaplan–Meier overall survival curves by ALDH1 expression. Five-year overall survival for ALDH1A1-positive and ALDH1A1-negative patients was 77.9% and 62.2%, respectively (*P*=0.002).
Abbreviation: ALDH1A1, aldehyde dehydrogenase 1A1.

poor survival,[26] and Chang et al demonstrated that ALDH1 expression correlated with a favorable prognosis in ovarian cancer,[27] being in line with our study results. It seems possible that one CSC marker from one organ or specific histology is not necessarily useful for identifying CSCs from other organs or histology. In lung ADC, ALDH1 may not be purely a CSC marker but the prognostic marker playing some pivotal role in biologic tumor behavior.

ALDH1A1-positive ADCs demonstrated a significant correlation with less poorly differentiated ADCs, and the frequency of ALDH1A1-positive tumors in papillary predominant ADCs was higher than in solid predominant ADCs.

Table 2 Multivariate analysis of overall survival

Variable	Hazard ratio	95% CI	*P*-value
Tumor size			
≤3.0 cm	1	1.017–3.546	0.044
>3.0 cm	1.899		
Lymph node metastasis			
Absent	1	1.354–5.392	0.005
Present	2.702		
Vascular invasion			
Absent	1	0.897–3.868	0.095
Present	1.863		
Pleural invasion			
Absent	1	0.873–3.831	0.110
Present	1.829		
ALDH1A1 expression			
<5% positive cells	3.218	1.674–6.188	<0.001
≥5% positive cells	1		

Abbreviations: ALDH1A1, aldehyde dehydrogenase 1A1; CI, confidence interval.

These results suggest that ALDH1A1 may play some role in essential morphogenic functions in lung ADC, and ALDH1A1-positive tumors may indicate lower biological aggressiveness.

Aldo-keto reductase (AKR) enzymes comprise a functionally diverse gene family.[28] In humans, four AKR1C isoforms have been identified. Of these, AK1C1 and AK1C3 are known to be cytosolic oxidoreductases that are involved in reduction of progesterone to the inactive form, 20-alpha hydroxyprogesterone, and the metabolism of steroids and prostaglandins with multispecificity, respectively.[29–31] Although neither CSC-related immunoreactivity marker had prognostic significance, predominantly solid ADCs had significantly higher expression of AK1C1 when compared with acinar or papillary predominant ADCs.

The prognostic value of the IASLC/ATS/ERS classification of lung ADC has been validated in several retrospective studies.[3,5–7] Yoshizawa et al recently reported a significant correlation between *EGFR* mutations and adenocarcinoma in situ/minimally invasive adenocarcinoma/lepidic/papillary subtypes, and *KRAS* mutation and mucinous subtypes.[6] Kadota et al demonstrated that immunoreactions of thyroid transcription factor-1 differ depending on the predominant structural subtype.[32] In the current study, the histologic subtype appeared to be correlated with specific CSC-related marker expression. The novel classification of lung ADC has important implications, not just for predicting patient prognosis, but also for genetic alterations and molecular biology, and